The Charged Higgs in Hadronic Decays With the ATLAS Detector

Kétévi Adiklè Assamagan
Hampton University, Hampton, VA 23668 USA

Abstract

The possibility of detecting the charged Higgs through its hadronic decay modes, using the ATLAS detector at the LHC is presented in this paper. Calculations are carried out in the context of the Minimal Supersymmetric Standard Model with the assumption that the mass scale of supersymmetric partners of ordinary matter is above the charged Higgs mass. For the charged Higgs mass below the top quark mass, the decay $H^{\pm} \rightarrow c\bar{s}$ can be used to determine the mass of the charged Higgs assuming it is discovered through other channels, for instance $H^{\pm} \rightarrow \tau\nu$, by observing the excess of τ production over the Standard Model prediction. Above the top quark mass, the charged Higgs can be detected through $H^{\pm} \rightarrow t\,b$ up to 400 GeV/c^2 for low or high $\tan\beta$ (< 2, or > 20).

1 Introduction

The Minimal Supersymmetric Standard Model (MSSM) predicts five physical states in the Higgs sector [1]. Two of these are charged conjugates of each other ($H^{\pm}$), the rest are neutral (h^0, H^0, and A^0). At tree level, all Higgs particle masses and couplings are determined by two parameters, generally taken as m_A, the mass of the CP-odd neutral Higgs A^0, and $\tan\beta$, the ratio of the vacuum expectation values of the Higgs doublets. Radiative corrections to the masses and the couplings have been accounted for in the present studies up to two-loop calculations. A central value of 175 GeV/c^2 was used for the top-quark mass.

In a model independent way, LEP2 has set lower limits on the mass of the charged Higgs boson, $m_{H\pm}$ ($57.5 - 59.5$ GeV/c^2) for any $\tan\beta$ [2]. CDF and DØ searched for $H^{\pm}$ in top decays using $p\bar{p} \rightarrow t\bar{t}$, with at least one of the top-quarks decaying via $t \rightarrow H^{\pm}b$ [3] [4]: a direct search of $H^{\pm}$ through the decay $H^{\pm} \rightarrow \tau\nu$ was carried out at high $\tan\beta$ (> 10), while at low $\tan\beta$ (< 1), due to large QCD background, an indirect search for the reaction $H^{\pm} \rightarrow c\bar{s}$ was performed. These searches excluded the low (< 1) and high (> 40) $\tan\beta$ regions almost up to the top quark mass [3]. DØ performed a disappearance search considering all the fermionic decay modes of the charged Higgs and improved upon previous limits in the $(m_{H\pm}, \tan\beta)$ parameter space [5].

In the study described herein, the charged Higgs discovery potential of the ATLAS detector in the (m_A, $\tan\beta$) parameter space has been investigated using the ATLFAST [6] and PYTHIA 5.7 [7] simulation packages. This is a particle-level simulation performed at $\sqrt{s} = 14$ TeV, but with the detector resolutions and efficiencies parametrized from full detector simulations. The discovery potential of two decay channels have been studied in detail as a function m_A and $\tan\beta$,

namely $H^{\pm} \to c\bar{s}$ ($m_{H\pm} < m_t - m_b$) and $H^{\pm} \to tb$ ($m_{H\pm} > m_t + m_b$). For each of these channels, the relevant background processes were also evaluated.

In the following sections, we present the details of our analysis of $H^{+} \to c\bar{s}$ and of $H^{\pm} \to tb$. Unless otherwise specified, the results shown here correspond to an integrated luminosity of 30 fb^{-1} for which we assume a b-tagging efficiency of 0.6 and a lepton detection efficiency of 0.9.

2 Branching Ratios

In the present study, we have assumed that the mass scale of supersymmetric partners of ordinary matter is above $m_{H^{\pm}}$ so that $H^{\pm}$ decays into the supersymmetric partners are forbidden [8]. The charged Higgs has several decay channels, two dominant ones being $H^{\pm} \to tb$ and $H^{\pm} \to \tau\nu$. Figure 1 summarizes the branching ratios of the four decay modes relevant to our analysis as a function $m_{H\pm}$ and for different values of $\tan\beta$. The data of Figure 1 are obtained from the HDECAY code [9]. For low $\tan\beta$ values, and mass below the top-quark mass, four channels have relatively high branching ratios; above the top-quark mass, the decay $H^{\pm} \to tb$ dominates. For high values of $\tan\beta$, and mass below the top-quark mass, the charged Higgs decays predominantly into the τ lepton; above, only the τ decays and $H^{\pm} \to tb$ have significant branching ratios.

3 Cross-sections

The search strategy is based on the $H^{\pm}$ production through the decay of the top quark, i.e., $t \to H^{\pm}b$ for $m_{H\pm} < m_t - m_b$. $t\bar{t}$ production is required with one of the tops decaying into the charged Higgs and the other decaying leptonically to provide the experimental trigger. The rate of the $t\bar{t}$ production with one of the tops decaying leptonically is $\sim$ 228 pb (assuming 590 pb for inclusive $t\bar{t}$

production). If the MSSM charged Higgs exists, the $t\bar{t}$ production rate, with both $t \to Wb$ decays is reduced. For instance, for $\tan\beta = 1.5$ and one top decaying leptonically, the expected rates are 170 pb and 90 pb for $m_{H\pm} = 110$ and 130 GeV/c^2 respectively. If such a substantial reduction of the expected $t\bar{t}$ cross-section can be observed, it could indicate the existence of the charged Higgs below the top-quark mass. The expected signal rates are shown in Table 1 as a function $m_{H\pm}$ for $\tan\beta = 1.5$.

Table 1: The expected rates ($\sigma \times BR$), for the signal $t\bar{t} \to bH^{\pm}Wb$ with $H^{\pm} \to c\bar{s}$ ($\tan\beta = 1.5$), and the $t\bar{t}$ background.

m_{H+} (GeV/c^2)	Signal Rate (pb)	Background Rate (pb)
110	1.7	170
130	0.7	90

Above $m_t + m_b$, we considered the single $H^{\pm}$ production through the process $gb \to t\,H^{\pm}$ followed by the $H^{\pm} \to tb$ decay. In this process, the charged Higgs is produced in association with a top quark. The final state therefore contains two top quarks, one of which is required to decay leptonically and the other hadronically. The rates for this process are shown in Table 2 as a function of $m_{H\pm}$ and $\tan\beta$.

Another production process of the charged Higgs is $gg \to H^{\pm}tb$. This process and the $gb \to H^{\pm}t$ process partially overlap so that when summing both contributions, care must be taken to avoid double counting [10]. When one requires three b-tagged jets — as is the case in this analysis — both processes will contribute to the total cross section. Theoretical calculations of the total cross-section as the sum of the contributions from the $2 \to 3$ and from the $2 \to 2$ processes are still in progress [11] [12].

Table 2: $\sigma \times$ BR(pb) for the signal $bg \to Ht \to l\nu bjjbb$ and the $t\bar{t}b + t\bar{t}q$ background as a function of $\tan\beta$.

Process	$m_{H\pm}$ (GeV/c^2)	$\tan\beta = 1.5$	$\tan\beta = 10$	$\tan\beta = 30$
$bg \to H^{\pm}t \to l\nu bjjbb$	200	3.4	0.4	1.6
	250	2.0	0.18	1.2
	300	1.2	0.14	1.0
	400	0.54	0.08	0.4
	500	0.3	0.04	0.2
$t\bar{t} \to jjbWb\,(W \to l\nu)$		228	228	228

4 The $t \to bH^{\pm} \to bc\bar{s}$ Channel

The $t\bar{t}$ events were generated through the processes $q\bar{q}$ (or gg) $\to t\bar{t}$ (PYTHIA subprocesses 81 and 82), with $t \to bH^{+} \to bc\bar{s}$ and $\bar{t} \to Wb \to l\nu b$. The main background for this process is just $t\bar{t}$ production with $t \to Wb \to jjb$ and $\bar{t} \to Wb \to l\nu b$. Table 1 shows the signal rates for $\tan\beta = 1.5$ and different values of $m_{H\pm}$. The selection conditions were two b-tagged jets (each with pseudo-rapidity $|\eta| < 2.5$ and transverse momentum $P_T > 15$ GeV/c) and a single isolated lepton ($|\eta| < 2.5$, $P_T^e > 20$ GeV/c or $P_T^{\mu} > 6$ GeV/c). For the events that passed the test, the $H^{\pm}$ mass peak was searched for in a di-jet reconstructed mass distribution, m_{jj}. The combinatorial background was reduced by applying a b-jet veto and a jet veto, i.e., only the presence of 2 additional non b-tagged jets (with $|\eta| < 2.0$) was allowed in addition to the isolated lepton and the two b-tagged jets. Other cuts were also considered as specified in Table 3. Figure 2 shows the di-jet mass distributions for the signal and the background for an integrated luminosity of 30 fb^{-1}. The expected sensitivities as a function of the cuts applied are shown in Table 3 for a mass window of $|m_{jj} - m_{H\pm}| < 2\sigma_{jj}$ ($\sigma_{jj} = 12$ GeV/c^2 is obtained from a Gaussian fit to the distribution of Figure 2,

Table 3: The estimated number of counts within the mass window of 130 ± 24 GeV/c^2 for low luminosity operation and for the specified cuts. C_0 = one lepton · 2b-jets · b-jet veto, $C_1 = C_0 \cdot$ jet veto, $C_2 = C_0 \cdot |\eta| < 5$, $C_3 = C_2 \cdot$ jet veto, $C_4 = C_0 \cdot |\eta| < 2$, $C_5 = C_4 \cdot$ jet veto, $C_6 = C_0 \cdot P_T > 30$ GeV, and $C_7 = C_6 \cdot$ jet veto.

Cuts	C_0	C_1	C_2	C_3	C_4	C_5	C_6	C_7
Signal ($\times 10^2$)	7.0	2.7	7.0	2.7	6.8	4.3	7.3	2.9
Background ($\times 10^4$)	3.4	0.5	3.4	0.5	2.8	0.9	3.1	0.5
S/B (%)	2.1	5.4	2.1	5.4	2.4	4.8	2.4	5.8
$S/\sqrt{B}$	3.8	3.8	3.8	4.0	4.0	4.5	4.1	4.1

top panel).

Table 4: The expected number of events for $H^{\pm} \to c\bar{s}$ within the mass window of $m_{H\pm} \pm 24$ GeV/c^2 for an integrated luminosity of 30 fb^{-1} and for the cuts C_3 and C_5 specified in Table 3; $\tan\beta = 1.5$.

	C_3	C_5	$m_{H\pm}$ (GeV/c^2)
Signal ($\times 10^2$)	5.3	8.7	110
Background ($\times 10^4$)	0.9	1.8	
S/B (%)	5.9	4.8	
$S/\sqrt{(B)}$	5.7	6.5	
Signal ($\times 10^2$)	2.7	4.3	130
Background ($\times 10^4$)	0.5	1.0	
S/B (%)	6.0	4.5	
$S/\sqrt{(B)}$	4.0	4.4	

In summary, assuming the charged Higgs is detected through $H^{\pm} \to \tau\nu$, by observing the excess of τ production over the Standard Model prediction, it might be possible to use this channel to measure $m_{H\pm}$. Table 4 shows the sensitivities and Figure 3 the expected signal and background distribution.

5 The $gb \rightarrow t\,H^{\pm} \rightarrow t\bar{t}b$ Channel

We used ATLFAST to study the possibility of detecting the charged-Higgs in the mass range $m_{H\pm} > m_t + m_b$. We've considered the production of the charged-Higgs through the reaction $gb \rightarrow tH^{\pm}$ (PYTHIA subprocess 161) with the charged-Higgs decaying via the channel $H^{\pm} \rightarrow tb$. Further, we assumed that both top quarks decay as follows: $t \rightarrow Wb$, with one of the W's decaying leptonically ($W \rightarrow l\nu$, $l = e, \mu$) and the other hadronically ($W \rightarrow jj$). The main background is coming from $t\bar{t}b$ and $t\bar{t}q$ production ($t\bar{t} \rightarrow WWbb \rightarrow l\nu jjbb$). We studied this channel for several values of $m_{H\pm}$ and $\tan\beta$ as shown in Table 2. To improve the signal to background ratio and the signal significance, the data were analyzed in the following sequence:

a) Search for an isolated lepton (an electron or a muon), three b-tagged jets and at least 2 non b-jets. For the lepton, we required $P_T^e > 20$ GeV/c and $P_T^{\mu} > 6$ GeV/c. We further required $P_T^j > 30$ GeV/c for all jets, including b-jets. We applied a pseudorapidity cut of $|\eta| < 2.5$ on b-jets.

b) Take the missing transverse momentum as the neutrino transverse momentum and fix the longitudinal component of the neutrino momentum by the W mass constraint. In general, this procedure gives two solutions both of which reconstruct the W mass. The event was rejected if this procedure did not yield any physical solution.

c) We considered all the possible non-b-jet combinations and demanded that the invariant masses m_{jj} be consistent with the W mass: $|m_{jj} - m_W| < 2\sigma_{jj}$, where $\sigma_{jj} \simeq 12.5$ GeV/c^2 is the resolution of the m_{jj} distribution (Figure 4). The 4-momenta of the jets which pass the m_{jj} mass cuts were rescaled to

give $m_{jj} = m_W$. The 3 b-jets can be paired in six different ways with the two W's to give top quark candidates. With the possible two solutions from the leptonic channel, there are up to nine reconstructed top quark masses for each jet-jet combination. We retained the pair of top quarks whose masses m_{jjb} and $m_{l\nu b}$ minimize the following:

$$(m_{jjb} - m_t)^2 + (m_{l\nu b} - m_t)^2, \tag{1}$$

d) Here too, we retain the events satisfying the mass cut: $|m_{jjb} - m_t| < 2\sigma$ and $|m_{l\nu b} - m_t| < 2\sigma$, where $\sigma = 12.5$ GeV/c^2 from the m_{jjb} and $m_{l\nu b}$ distributions. The 4-momenta of the top quark pairs retained in **c)** were rescaled such that $m_{jjb} = m_t$ and $m_{l\nu b} = m_t$. The remaining b-quark can pair with one of the reconstructed top-quarks to give a charged Higgs candidate. Since there are no clear criteria to select the right (tb) combination, we retained both choices. Thus the signal events contain a combinatorial background as shown in Figure 5 (keyhad=0) and Figure 6 (keyhad=3). The correct pairing would give a peak at $m_{H^{\pm}}$ in the mass distribution as shown in Figure 7 (keyhad=3).

e) A final cut on the transverse momenta of the reconstructed charged Higgs and top candidates (80 and 60 GeV/c respectively) was applied to improve the reconstruction.

Table 5 lists the efficiency of the cuts **a)** through **d)** for the signal and the background.

To reduce (or eliminate) the combinatorial background coming from incorrect (tb) pairings, we examined the kinematics of the the reaction $gb \to t\,H^{\pm} \to jjl\nu bbb$ with the hope of finding a set of cuts which will increase the fraction of correct (tb) selections. The cuts considered were:

Table 5: Efficiency of the cuts **a)**, **b)**, **c)** and **d)** for the signal and the background.

Process	$m_{H\pm}$ (GeV/c^2)	**a)**	**b)**	**c)**	**d)**
$bg \to Ht \to l\nu bjjbb$	200	2.5%	1.9%	1.3%	1.0%
	300	4.5%	3.4%	2.3%	1.7%
	400	5.0%	3.6%	2.5%	1.7%
	500	5.1%	3.6%	2.6%	1.7%
$t\bar{t} \to jjbWb\,(W \to l\nu)$		0.1%	0.1%	0.06%	0.05%

- The cone between the charged Higgs and its associated top: in hard scattering, the charged Higgs and its associated top are produced back to back. Therefore, one can select the correct $H^{\pm}$ candidate by requiring the largest cone between the charged Higgs and its associated top. However, this cut is rendered effectively useless by initial state radiations.

- The cone between the top and the b-quarks from the decay of the charged Higgs may be required to be the smallest for the selection of the correct $H^{\pm}$ candidate. But then again, this would work only in hard scattering.

- We also explored other reconstruction procedures. For instance, instead of minimizing for a pair of tops and then reconstructing two charged Higgs candidates, one can reconstruct all the charged Higgs candidates for each event and retain the one whose top decay best reconstructs m_t.

Thus far, no set of cuts nor reconstruction technique have been found which unambiguously identify the correct (tb) from the decay of the charged Higgs. The procedure described in this paper is flawed in 2 ways. First, in minimizing for a pair of tops, one might select the wrong $W \to jj$. Second, the remaining b-jet that is paired to the tops to obtain the $H^{\pm}$ candidates could also be the wrong one. Indeed, as can be seen from Table 6, our reconstruction procedure is

Table 6: Efficiency of the reconstruction algorithm for correctly reconstructed top-quarks and charged Higgs after all cuts including $P_T^t > 60$ GeV/c and $P_T^{H^{\pm}} > 80$ GeV/c. Keyhad is a switch in ATLFAST indicating the physics process considered in the simulation: keyhad=0 (hard scattering), keyhad=1 (plus initial state radiations), keyhad=2 (plus final state radiations), and keyhad=3 (plus multi-interactions and hadronizations).

Keyhad	0	1	2	3
$m_{H^{\pm}} = 200$ GeV/c^2	0.87			0.48
$m_{H^{\pm}} = 300$	0.80	0.62	0.46	0.46
$m_{H^{\pm}} = 400$	0.89			0.59
$m_{H^{\pm}} = 500$	0.93			0.65

at best 65% efficient in reconstructing correctly the right top and b-quarks from $H^{\pm} \to tb$. The correctly reconstructed event was defined as follows:

- If the charged Higgs decays leptonically, then the charge of the decay lepton is opposite to that of the charged Higgs itself. This was used to trace back the top from $H^{\pm} \to tb$.

- To identify the correct b-jet from the same decay, we first identified the correct b-quark from the particle table (PYTHIA outputs). Then the correct b-jet is that which minimizes the cone

$$\Delta R = \sqrt{\Delta\theta^2 + \Delta\phi^2}. \tag{2}$$

- The data of Table 6 are the fractions of the events for which the reconstruction procedure gets the correct (tb) combinations obtained as described above.

Figure 7 shows the expected improvement in the signal reconstruction if the right top-quark and the right b-quark from the charged Higgs decay were identified correctly with a 100% efficiency, in which case, 86% of the events are within a mass window of $\pm 2\sigma = \pm 34$ GeV/c^2 for $m_{H^{\pm}} = 300$ GeV/c^2.

Above $m_{H\pm} = 300$ GeV/c^2, the reduced signal rate and the combinatorial background render the observation of this channel difficult. Below 300 GeV/c^2, it is possible to observe a clear signature above the background: Figure 8 shows the expected statistical fluctuations on the data after all the cuts discussed here and for an integrated luminosity of 30 fb^{-1}. The results of Figure 8 were obtained by first fitting the data to a Gaussian (the signal) and an exponential (the background) functions. The results of the fit were then smeared with a random Gaussian function to obtain the expected statistical fluctuations of the data. Table 7 shows the expected signal to background ratio and the significance for $m_{H\pm} = 200 - 400$ GeV/c^2.

Table 7: Expected resolutions and peak positions for the reconstructed m_{tb} distributions, number of signal and background events inside $\pm 2\sigma$ mass window, and signal to background ratios and signal significances for $\tan\beta = 1.5$ and for $< m_0 > -2\,\sigma \;< m_{H\pm} < \;< m_0 > +2\,\sigma$, where the mean $< m_0 >$ and the standard deviation σ were obtained from the fit.

$m_{H\pm}$ (GeV/c^2)	200	250	300	400
$< m_0 >$ (GeV/c^2)	215	265	303	393
σ (GeV/c^2)	15	37	39	49
Signal events	300	560	378	152
Acceptance (%)	42	71	73	64
$t\bar{t}$ events	760	1590	1650	1270
S/B	0.4	0.36	0.22	0.12
$S/\sqrt{B}$	10.9	14.0	9.3	4.3

In summary, we have searched for the possibility of detecting the charged Higgs in the mass region above the top mass. We considered the charged Higgs production through the reaction $gb \to H^{\pm}t$ with the charged Higgs decaying via $H^{\pm} \to tb$. One of the tops decays leptonically to trigger the experiment and the other hadronically. The background process considered for this reaction are $t\bar{t}b$ and $t\bar{t}q$ productions. The data was analyzed by requesting 3 b-tagged jets,

one isolated lepton and at least 2 additional jets. In the leptonic channel, the missing traverse momentum was taken as the neutrino transverse momentum and the longitudinal component of the neutrino momentum was fixed by the W mass constraint. In the hadronic channel, all the jet-jet combinations whose invariant masses were consistent with the W mass were considered. All the possible top candidates were then reconstructed and a pair of tops was selected based on a chi-square criterion. The remaining b-jet could be paired with either top to produce two charged Higgs candidates. We examined the kinematics of the production and the decays with the hope of finding some cuts which could help select the correct charged Higgs candidate. No such cuts have been found and we were forced to accept the two solutions with one leading to a combinatorial background in addition to the physics $t\bar{t}b$ and $t\bar{t}q$ backgrounds. We also explored other reconstruction methods without much success. The current results suggest that above $m_{H^{\pm}} = 300$ GeV/c^2, the reduced signal rate and the combinatorial

Table 8: Sensitivity of the ATLAS detector ($S/\sqrt{B}$) to the observation of the charged Higgs through $H^{\pm} \to tb$. Discovery is possible in the low (< 2.5) and the high (> 25) $\tan\beta$ regions up to 400 GeV/c^2.

$m_{H^{\pm}}$ (GeV/c^2)	$\tan\beta = 1$	$\tan\beta = 2$	$\tan\beta = 10$	$\tan\beta = 25$	$\tan\beta = 35$
200	11.5	5.3	1.3	2.9	5.5
250	19.6	6.1	1.1	5.1	11.1
300	13.8	5.2	1.1	4.9	9.9
400	7.7	2.8	0.5	2.3	4.7

background make the observation of this channel difficult. Below the charged Higgs mass of 300 GeV/c^2, this channel may be observed above the $t\bar{t}b$ plus $t\bar{t}q$ background. Our results for $m_{H^{\pm}} = 200 - 400$ GeV/c^2 are summarized in Table 7 and shown in Figure 8. At high values of $\tan\beta$, sensitivity is expected up to 400 GeV/c^2 as shown in Table 8 and Figure 9. A reconstruction algorithm or

a set of cuts which can unambiguously select the correct (tb) pairing from the decay of the charged Higgs out of all the possible (tb) candidates, would lead to significant improvement in the signal to background ratios and significances, especially in the intermediate $\tan\beta$ region $(2-25)$.

6 Conclusions

We have studied the charged Higgs discovery potential of the ATLAS detector. Two hadronic decay channels of the charged Higgs have been investigated in the (m_A, $\tan\beta$) parameter space, namely $H^{\pm} \rightarrow c\bar{s}$ below m_t, and $H^{\pm} \rightarrow tb$ above m_t. Our analyses were performed at the particle level using the ATLFAST and PYTHIA 5.7 codes. The ATLFAST code integrates major detector performance parameters such as resolutions and efficiencies in the analysis. Our results suggest that for $m_{H^{\pm}} < m_t - m_b$, the reaction $H^{\pm} \rightarrow c\bar{s}$ can be used to determine $m_{H^{\pm}}$ assuming the charged Higgs is discovered through other channels, namely by observing the excess of τ production above Standard Model expectation. Above the top quark mass, the channel $H^{\pm} \rightarrow tb$ becomes the main decay mode particularly at low $\tan\beta$ and discovery is possible through this channel up to $m_{H^{\pm}} = 300$ GeV/c^2. For $m_{H^{\pm}} > 300$ GeV/c^2, the combinatorial background and the reduced signal rates render the observation of this channel extremely difficult. However, detection is still possible at high values of $\tan\beta$ (> 25) for $m_{H^{\pm}} \leq 400$ GeV/c^2.

Acknowledgements

The author expresses immense gratitude to E. Richter-Wąs for fruitful discussions and constructive criticisms. The present work is supported by a grant from the USA National Science Foundation (grant number 9722827).

References

[1] P. H. Nilles, *Phys. Rev.* **110**, 1 (1984); H. Haber and G. Kane, *Phys. Rev.* **115**, 75 (1985).

[2] ALEPH Collaboration, CERN-EP/99-01; L3 Collaboration, CERN-EP/98-149; OPAL Collaboration, CERN-EP/98-173.

[3] L. Groer for CDF and DØ Collaborations, hep-ex/9707034.

[4] CDF Collaboration, *Phys. Rev. Lett.* **79**, 357 (1997).

[5] DØ Collaboration, hep-ex/9902028.

[6] E. Richter-Wąs, D. Froidevaux and L. Poggioli, ATLAS Internal Note, PHYS-No-079 (1996).

[7] T. Sjöstrand, "High-Energy Physics Event Generation with PYTHIA 5.7 and JETSET 7.4", CERN preprints-TH.7111/93 and CERN-TH.7112/93, Comp. Phys. Comm. **82** (1994) 74.

[8] E. Richter-Wąs et al, *Inter. Journ. of Mod. Phys. A*, **Vol. 13, No.9**, 1371 (1998).

[9] A. Djouadi, J. Kalinowski and M. Spira, Comp. Phys. Comm. **108** (1998) 56.

[10] F. Borzumati, J.-L. Kneur, and N. Polonsky, CERN-TH/99-118, PM/98-38, RU-98-45, hep-ph/9905443.

[11] J.-L. Kneur, S. Moretti, D. P. Roy, private communication.

[12] D. P. Roy, private communication.

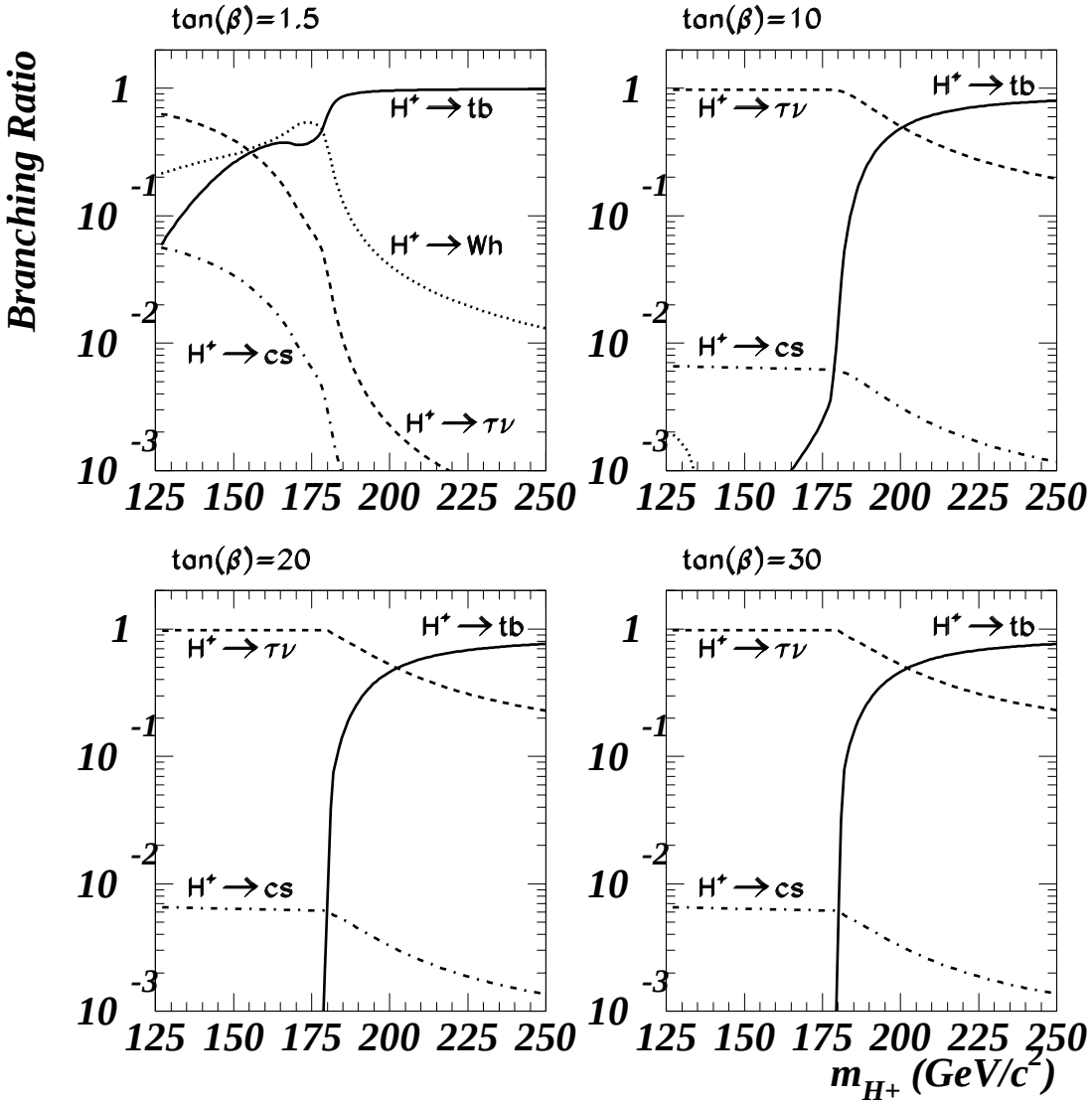

Figure 1: The branching ratios of $H^{\pm}$ decays as a function of $m_{H\pm}$ and for different values of $\tan\beta$. Only the relevant decay modes are shown here. The two most dominant decay channels over most of the range are $H^{\pm} \to \tau\nu$ and $H^{\pm} \to tb$.

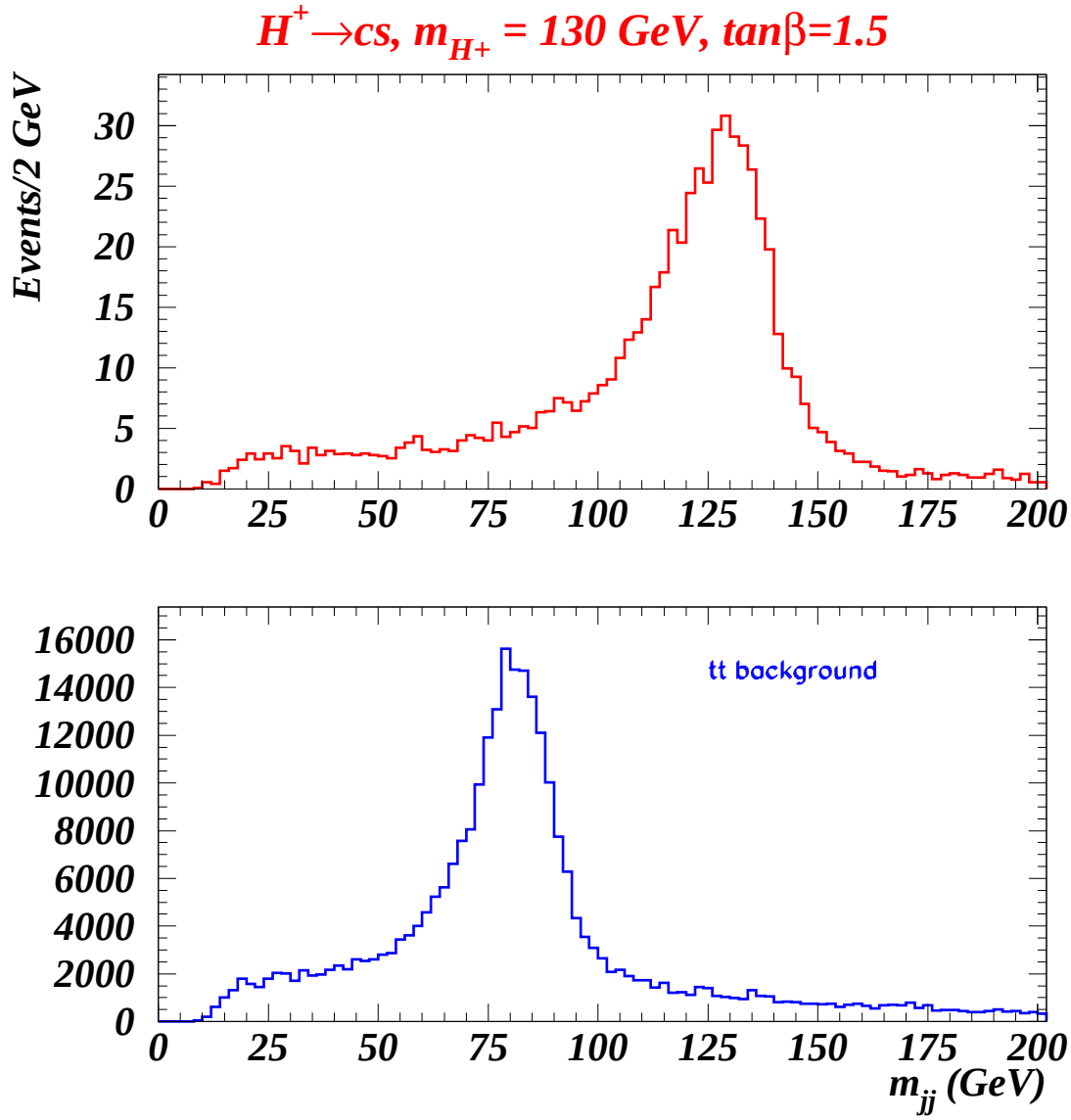

Figure 2: The di-jet reconstructed mass distribution for the signal events, $t\bar{t} \to bH^+Wb\,(W \to l\nu)$ and $H^\pm \to c\bar{s}$. After applying jet veto on the third jet, the $H^\pm$ mass peak can be seen in the m_{jj} distribution. The bottom panel is the m_{jj} distribution for the $t\bar{t}$ background events.

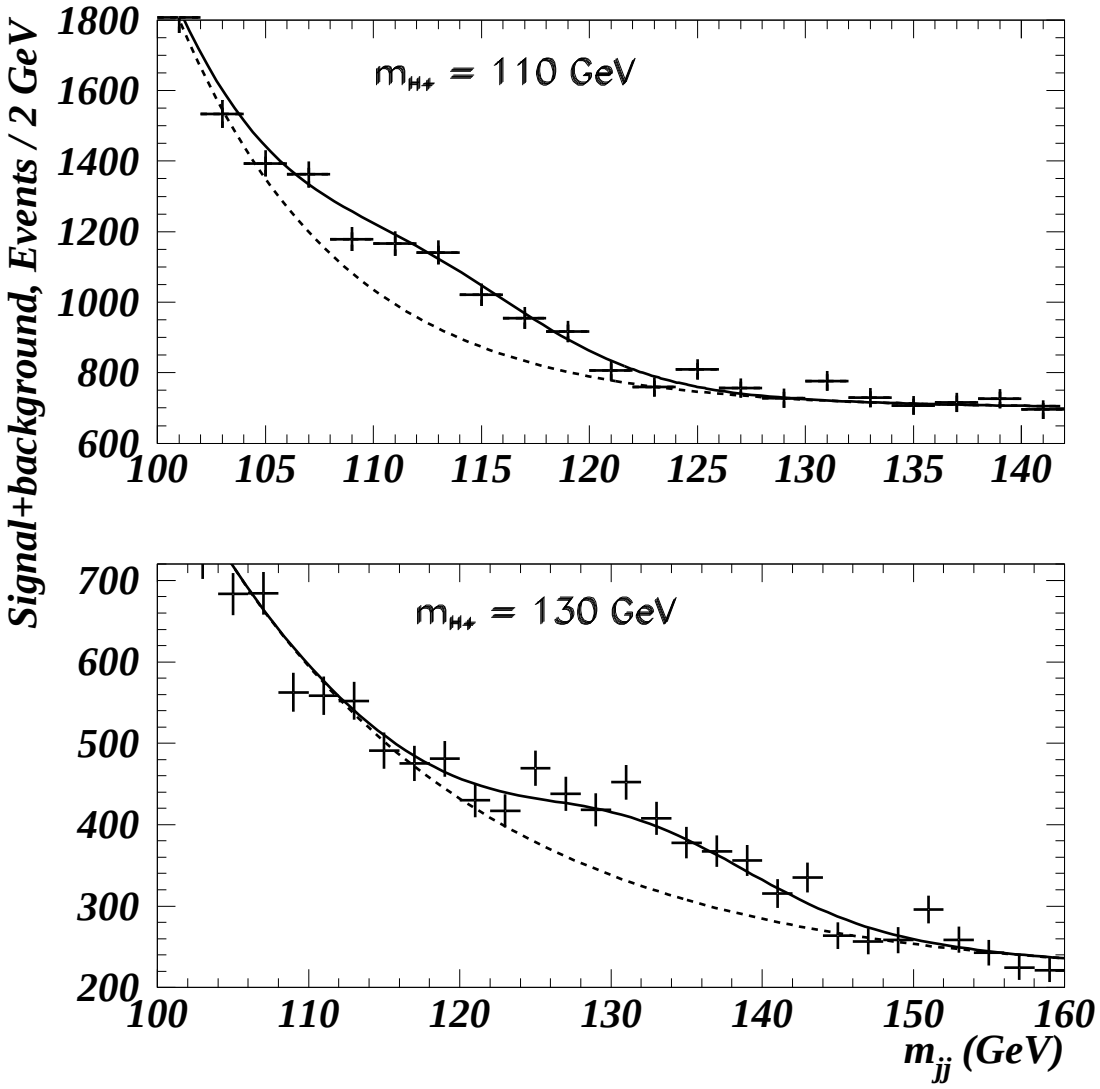

Figure 3: For the $H^{\pm} \to c\bar{s}$ channel, the expected m_{jj} distributions from the signal plus background (solid) and from the background (dashed) for $m_{H^{\pm}} = 110$ and 130 GeV/c^2, $\tan\beta = 1.5$ and for an integrated luminosity of 30 fb^{-1}. The errors are statistical only.

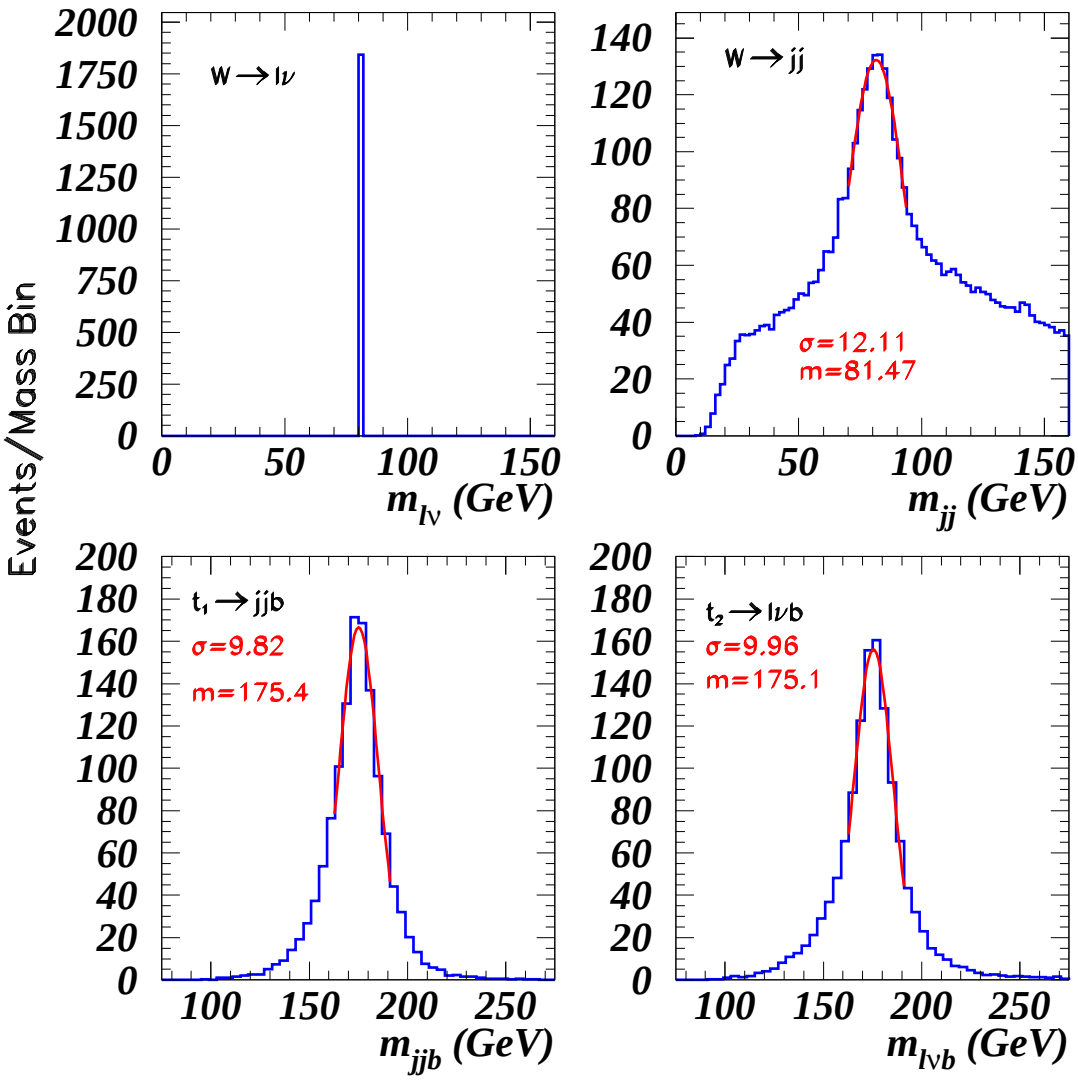

Figure 4: The reconstructed mass distributions $m_{l\nu}$, m_{jj}, m_{jjb} and $m_{l\nu b}$ for the channel $bg \to Ht \to l\nu bjjbb$ for $m_{H^\pm} = 200$ GeV/c^2.

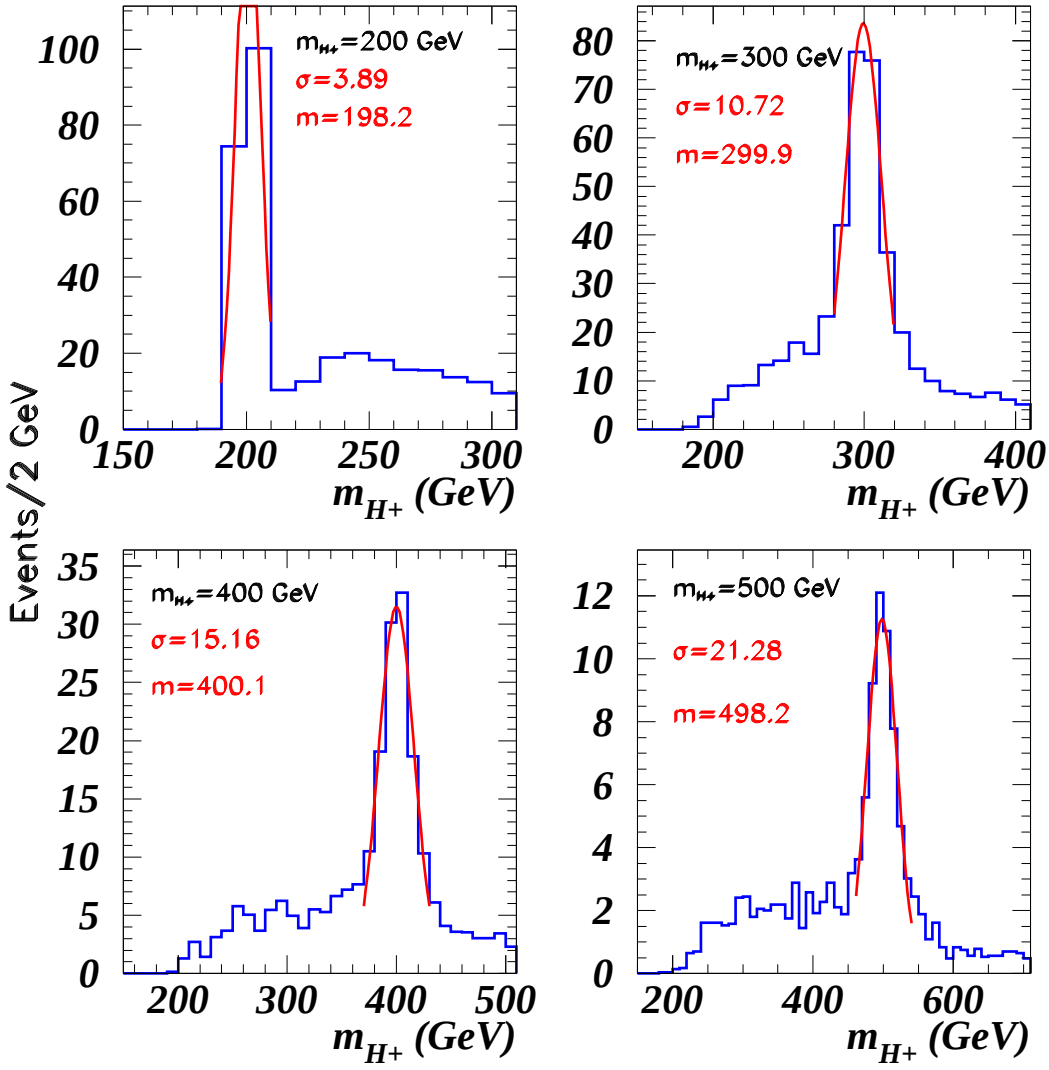

Figure 5: The reconstructed charged-Higgs mass distribution for the signal $bg \to H^{\pm}t \to l\nu bjjbb$. Only hard scattering is considered here. The correct pairing of the remaining b-quark to one of the two tops gives a peak at $m_{H^{\pm}}$ while the incorrect pairing gives a broad spectrum.

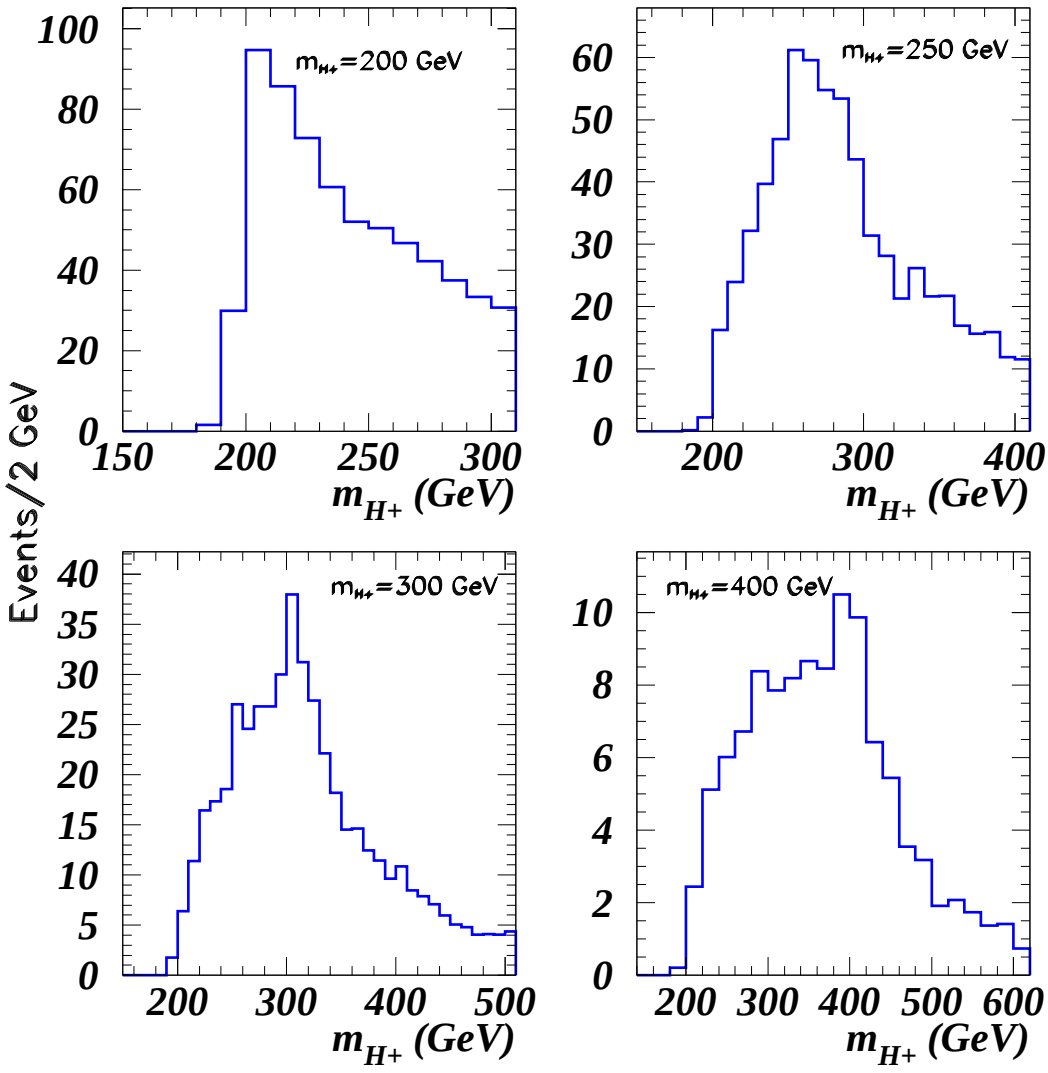

Figure 6: The reconstructed charged-Higgs mass distribution for the signal $bg \to H^{\pm}t \to l\nu bjjbb$. Initial and final state radiations, multi-interactions and hadronizations are included. The two possible choices of reconstructed $m_{H^{\pm}}$ are retained with the wrong combination leading to a combinatorial background from signal events.

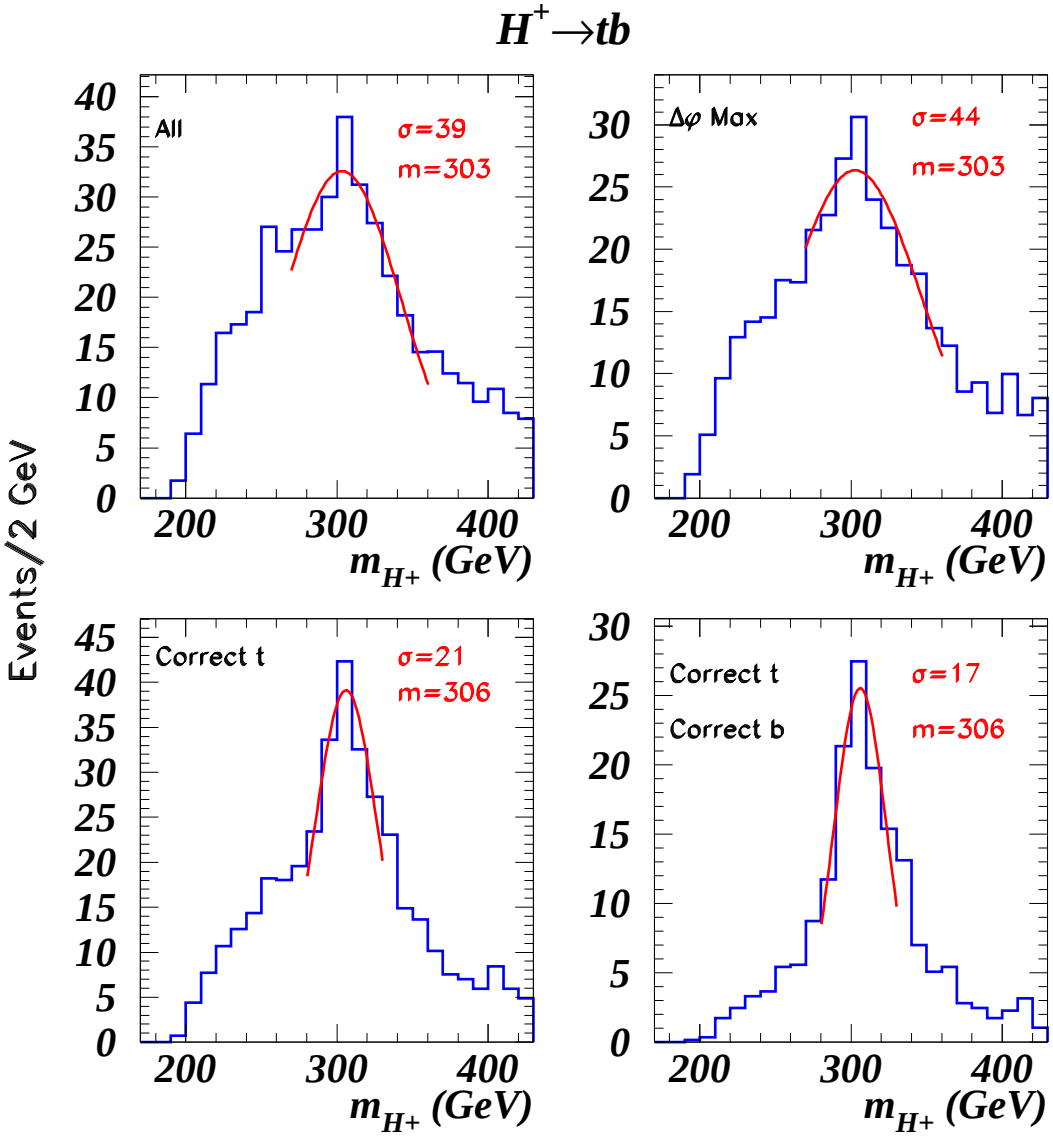

Figure 7: Expected improvement in the reconstruction if the right top and b-quarks were selected correctly. In the top left panel, we accepted both $H^{\pm}$ candidates. In the top right panel, we accepted the $H^{\pm}$ having the largest opening angle with the associated top from $gb \rightarrow H^{\pm}t$. Initial state radiations render this kinematical cut inefficient. The bottom left panel is the improvement over the top left panel if the top-quark from the decay of the charged Higgs were selected correctly in the reconstruction. The bottom right panel is the further improvement over the bottom left panel if in addition, the b-jet from the $H^{\pm}$ decay were also selected correctly. The data shown here is for $m_{H^{\pm}} = 300$ GeV/c^2.

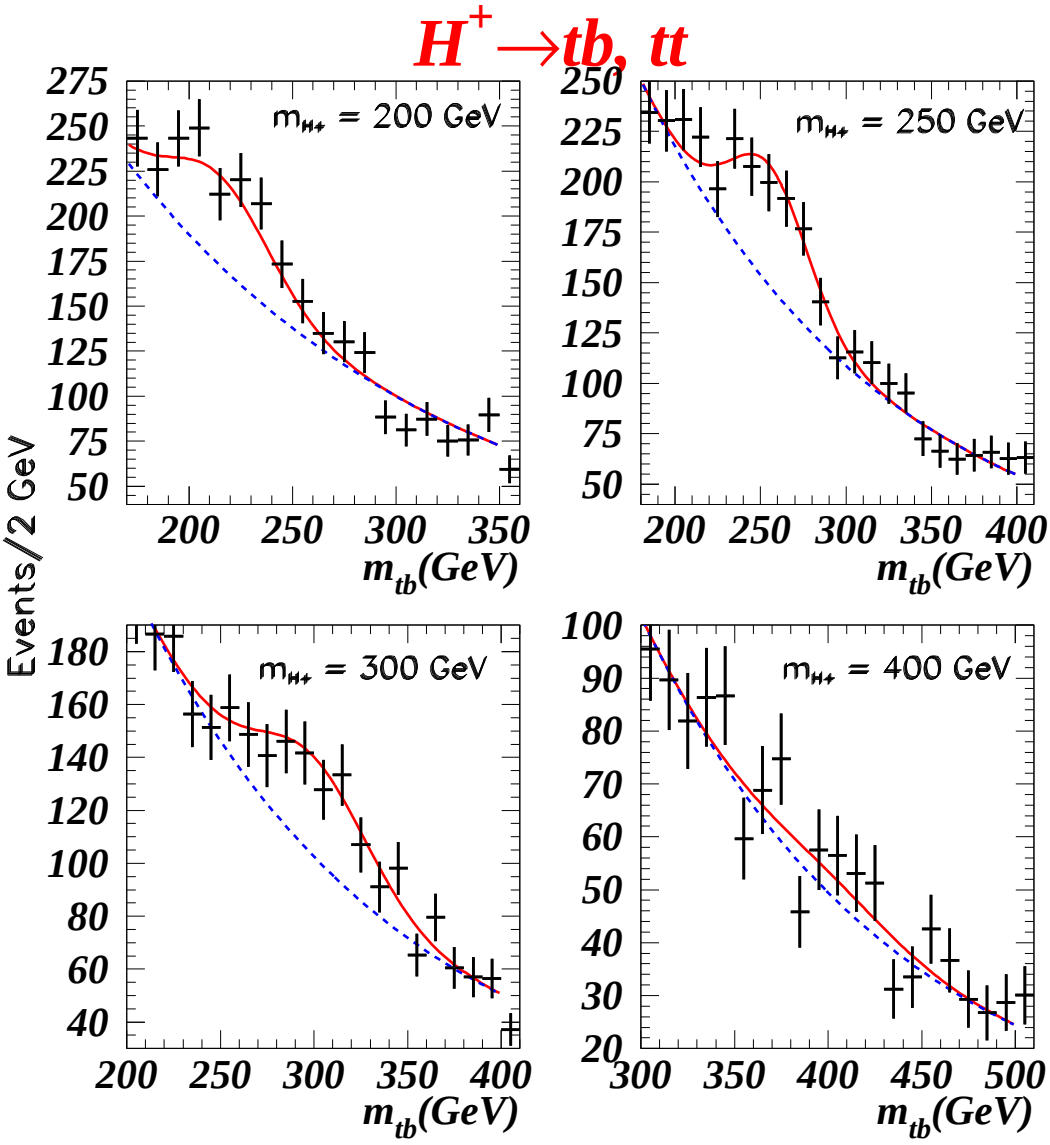

Figure 8: The signal plus background (solid) and the background (dashed) distributions for the reconstructed invariant mass m_{tb} of a Higgs mass of 200, 250, 300 and 400 GeV/c^2, $\tan\beta = 1.5$ and an integrated luminosity of 30 fb^{-1}. The errors are statistical only.

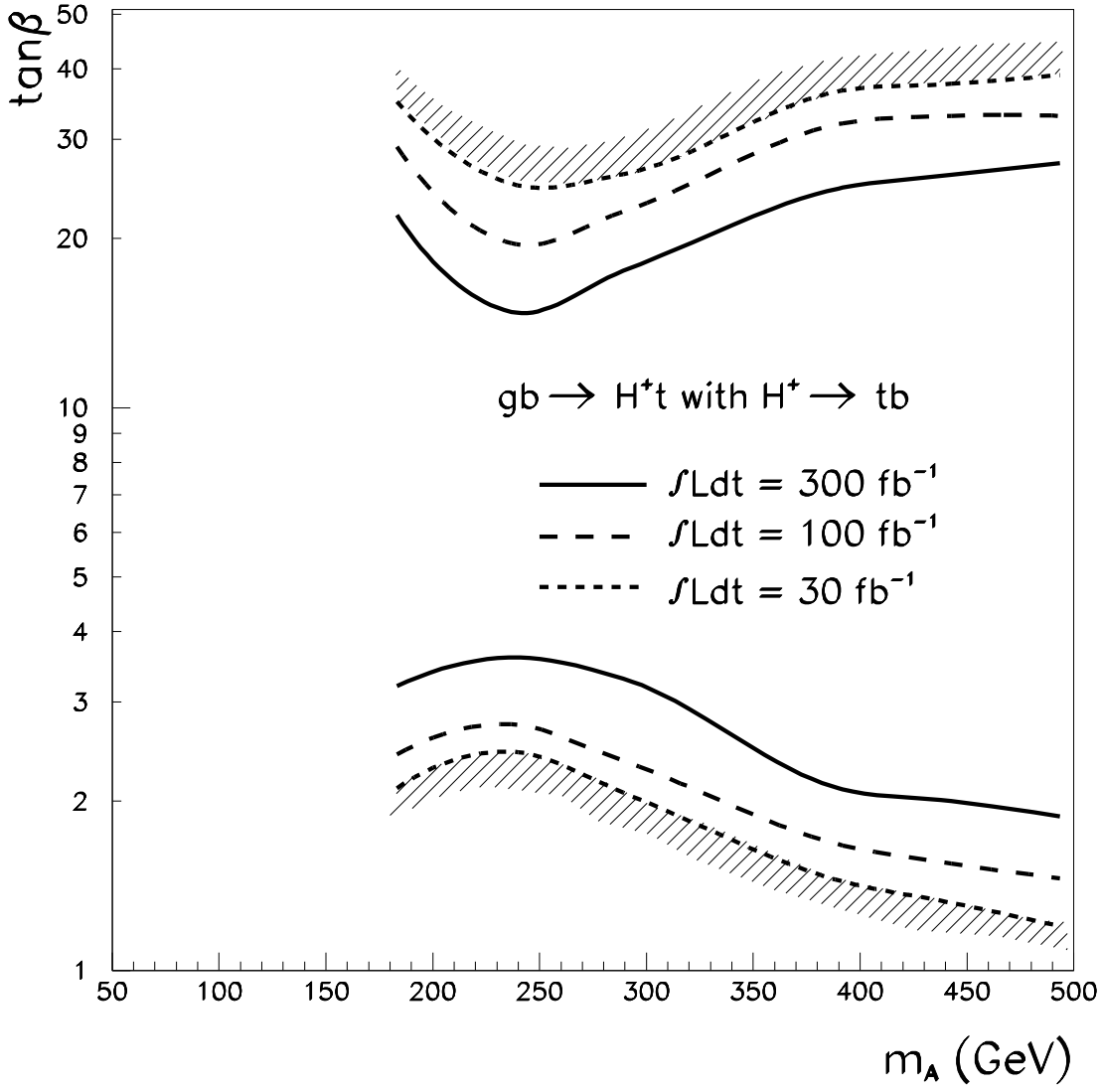

Figure 9: For integrated luminosities of 30, 100 and 300 fb^{-1}, the 5σ-discovery contour curves for the $H^{\pm} \to tb$ channel in the $(m_A, \tan\beta)$ plane.